Acta Chemica Scandinavica A 39 (1985) 199–207

Magnetic and Structural Properties of Transition Metal Substituted MnP. VI. $Mn_{1-t}Mo_tP$ and $Mn_{1-t}W_tP$

HELMER FJELLVÅG and ARNE KJEKSHUS

Kjemisk Institutt, Universitetet i Oslo, Blindern, Oslo 3, Norway

$Mn_{1-t}Mo_tP$ and $Mn_{1-t}W_tP$ are studied by X-ray and neutron diffraction and magnetic susceptibility measurements between 10 and 1000 K. The ferromagnetic (F) state of MnP probably extends up to $t \approx 0.08$ for $Mn_{1-t}W_tP$, where F, para- (P) and helimagnetic (H_c) phases very likely meet in a triple point of the magnetic phase diagram. The H_c state exists to $t \geqq 0.20$. A similar situation prevails for $Mn_{1-t}Mo_tP$. The results are discussed in relation to the findings for the $Mn_{1-t}T_tP$; T=3*d* metal phases.

The preceding papers of this series[1–6] on pseudo binary $Mn_{1-t}T_tP$ phases have been concerned with 3*d* metals (T=V, Cr, Fe, Co and Ni) as substituents for Mn. The present contribution gives an account of structural and magnetic data obtained for T=Mo and W.

The distinction in crystal structure between MoP (WC type[7]) and WP (MnP type[8]) is reflected in the limited miscibility of the MnP–MoP system. According to the partly unpublished thesis of Guerin[9] (see also Ref. 10), $Mn_{1-t}Mo_tP$ has a miscibility gap for $\sim 0.33 < t < \sim 0.85$ whereas $Mn_{1-t}W_tP$ exhibits complete solid solubility. The magnetic properties which have been unveiled for $Mn_{1-t}T_tP$ with T=3*d* metal, raise some interesting questions for T=Mo and W, *inter alia*:

(i) Will the para- (P), ferro- (F) and helimagnetic (H_c) states of MnP (*cf.*, *e.g.*, Ref. 2) also extend appreciably into the ternary region of $Mn_{1-t}Mo_tP$ and $Mn_{1-t}W_tP$?

(ii) Will the P, F and H_c phases of $Mn_{1-t}Mo_tP$ and/or $Mn_{1-t}W_tP$ meet in a triple point of the *t*,T phase diagram?

(iii) Will the relative magnetic moment (μ/μ_{MnP}) and Curie temperature ($T_C/T_{C,MnP}$) obey the same correlation[1,6] with the difference in the number of outer electrons ($\Delta n = n_{Mn_{1-t}T_tP} - n_{MnP}$) as found for the 3*d* T metals?

EXPERIMENTAL

Samples were made from initial batches of MnP and MoP or WP, preparational details concerning the former being given in Ref. 2. MoP and WP were made from 99.95 % Mo and W (Koch-Light Laboratories; powder) and 99.999 % P (Koch-Light Laboratories; lumps of red P). Stoichiometric quantities of the elements were heated in evacuated, sealed quartz tubes. These were placed in horizontally positioned furnaces and the temperature was slowly increased (3×40 and 3×100 °C per d for MoP and WP, respectively) to 1000 °C, kept there for 2 d and cooled to room temperature over 1 d. After careful grinding the samples were subjected to similar heat treatments. MnP and MoP or WP were mixed in proportions

0302-4377/85 $2.50

appropriate to the desired ternary compositions and subjected to three heat treatments (intermediate grindings) at 1000–1050 °C for 7 d, and finally cooled to room temperature over 1 d.

Experimental details concerning powder X-ray and neutron diffraction and magnetic susceptibility measurements are given in Ref. 11. The nuclear neutron scattering lengths (in 10^{-12} cm) $b_{Mn}=-0.37$, $b_{Mo}=0.69$, $b_W=0.48$ and $b_P=0.51$ were taken from Ref. 12, and the magnetic form factor for Mn^{2+} from Ref. 13.

RESULTS AND DISCUSSION

(i) *Homogeneity ranges and atomic arrangement.* The present findings concur with those of Guerin[9] (see also Ref. 10) in that a miscibility gap $0.38\pm0.04 \leqq t \leqq 0.80\pm0.05$ for $Mn_{1-t}Mo_tP$ and a complete solid solubility for $Mn_{1-t}W_tP$ have been confirmed. The MnP type structure (here using the *Pnma* setting, $c>a>b$) is found for $Mn_{1-t}Mo_tP$ with $0.00 \leqq t \leqq 0.38\pm0.04$ and the entire composition range of $Mn_{1-t}W_tP$. $Mn_{1-t}Mo_tP$ with $0.80\pm0.05 \leqq t \leqq 1.00$ takes the WC type structure. The present results are also in these respects in excellent agreement with those of Guerin.[9]

Fig. 1 shows the compositional variation of the room temperature unit cell dimensions for $Mn_{1-t}Mo_tP$ and $Mn_{1-t}W_tP$ as determined by the X-ray diffraction (Guinier) technique. The illustration covers only the Mn rich regions ($0.00 \leqq t \leqq 0.30$) which are the most relevant

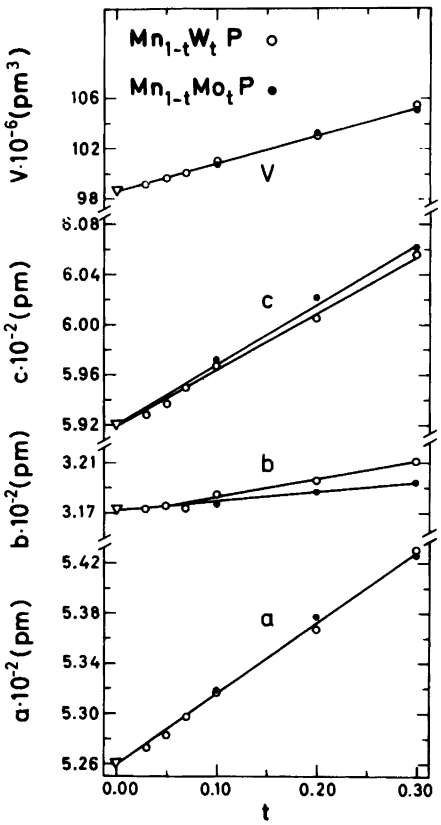

Fig. 1. Unit cell dimensions of $Mn_{1-t}Mo_tP$ and $Mn_{1-t}W_tP$ *versus* t (for $0.00 \leqq t \leqq 0.30$) at 293 K. Legends to symbols are given on the illustration. *Calculated* error limits do not exceed twice the size of symbols. (1 Å=10^2 pm.)

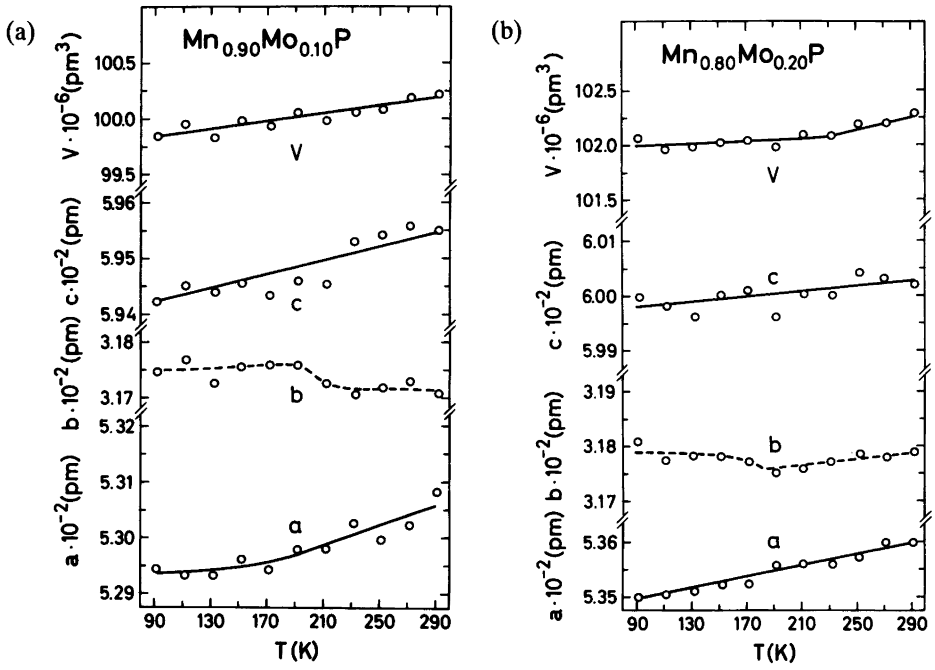

Fig. 2. Unit cell dimensions *versus* temperature for (a) $Mn_{0.90}Mo_{0.10}P$ and (b) $Mn_{0.80}Mo_{0.20}P$. *Calculated* error limits do not exceed twice the size of symbols. (1 Å=10^2 pm.)

to the magnetic features of these phases. Fig. 1 brings out a very close correspondence between the compositional variations of the unit cell dimensions of $Mn_{1-t}Mo_tP$ and $Mn_{1-t}W_tP$. The unit cell dimensions reported by Guerin[9] for the Mn rich regions of $Mn_{1-t}Mo_tP$ and $Mn_{1-t}W_tP$ differ somewhat from those presented in Fig. 1. The distinctions are most pronounced for MnP itself where Guerin obtained a=524.0, b=316.5 and c=591.0 pm as opposed to a=526.01(4), b=317.41(2) and c=591.93(4) pm in the present study. The present data are, on the other hand, in excellent agreement with those in Refs. 8,14. A methodological explanation of this discrepancy appears to be less likely since the differences between the two studies vary with the composition (t). [For MoP and WP there are, *e.g.*, excellent agreement; a=322.3 and c=319.1 pm *versus* a=322.21(3) and c=319.15(4) pm and a=573.0, b=324.9 and c=622.1 pm *versus* a=573.37(7), b=325.00(4) and c=622.12(10) pm are found by Guerin[9] and in the present study, respectively.]

The X-ray and neutron diffraction data substantiate that $Mn_{1-t}Mo_tP$ ($0.00 \leqq t \leqq 0.38 \pm 0.04$) and $Mn_{1-t}W_tP$ ($0.00 \leqq t \leqq 1.00$) adopt the MnP type structure with long range, random distribution of Mn and Mo or W over the metal sub-lattice. The unit cell dimensions and positional parameters, as derived from the powder neutron diffraction data for $Mn_{0.90}Mo_{0.10}P$, $Mn_{0.90}W_{0.10}P$ and $Mn_{0.80}W_{0.20}P$, are listed in Table 1. The slightly larger scatter of the data in Table 1 compared with the smooth curves in Fig. 1 is attributed to methodology of the neutron diffraction technique. The data for the unit cell dimensions at 293 and 10 K in Table 1 show only very vague indication of the occurrence of co-operative magnetism in $Mn_{1-t}Mo_tP$ and $Mn_{1-t}W_tP$ [see (iii)]. This feature is also reflected in Fig. 2

Table 1. Unit cell dimensions and positional parameters with standard deviations for $Mn_{1-t}Mo_tP$ and $Mn_{1-t}W_tP$ as derived by Rietveld analysis of powder neutron diffraction data. Space group *Pnma*; Mn/Mo or Mn/W in 4*c* and P in 4*c*. (Nuclear R_n-factors ranging between 0.03 and 0.06; profile R_p-factors ranging between 0.08 and 0.15; 20–25 nuclear reflections.)

T	*t*	T (K)	*a* (pm)	*b* (pm)	*c* (pm)	x_T	z_T	x_P	z_P
Mo	0.10	293	530.83(5)	317.96(3)	596.05(5)	−0.0004(36)	0.2010(35)	0.1881(16)	0.5684(13)
		150	529.54(6)	318.43(3)	595.06(6)	−0.0007(46)	0.2031(44)	0.1861(20)	0.5699(16)
		10	529.31(6)	318.40(3)	594.60(7)	0.0013(47)	0.2055(46)	0.1869(23)	0.5703(16)
W	0.10	293	531.85(6)	319.00(3)	595.86(6)	0.0046(31)	0.1992(25)	0.1885(19)	0.5696(16)
		10	530.14(6)	319.17(3)	594.30(7)	0.0043(26)	0.1978(30)	0.1865(23)	0.5686(17)
	0.20	293	537.76(7)	320.28(4)	600.86(7)	0.0006(46)	0.1976(44)	0.1890(17)	0.5673(15)
		10	536.31(6)	320.14(3)	599.50(6)	0.0028(49)	0.1993(43)	0.1878(16)	0.5667(13)

which gives the temperature variations of the unit cell dimensions of $Mn_{0.90}Mo_{0.10}P$ and $Mn_{0.80}Mo_{0.20}P$ (90–290 K) as typical examples of the results obtained for various compositions ($t \neq 0$). This distinguishes these phases from the other $Mn_{1-t}T_tP$ phases we have studied,[2–6] which generally show a fairly marked kink point on the thermal expansion curve for b within some 20–50 K of the co-operative to paramagnetic phase transition.

The positional parameters for $Mn_{1-t}Mo_tP$ and $Mn_{1-t}W_tP$ (Table 1) are constant within two calculated standard deviations for $0.00 \leqq t \leqq 0.20$ and $10 \leqq T \leqq 293$ K in line with the findings for the $Mn_{1-t}T_tP$ phases with $T=3d$ metal.

(ii) *Magnetic susceptibility.* The reciprocal magnetic susceptibility *versus* temperature curves for $Mn_{1-t}Mo_tP$ ($0.00 < t \leqq 0.30$) and $Mn_{1-t}W_tP$ ($0.00 < t \leqq 0.50$) in Fig. 3 fit into the pattern of other $Mn_{1-t}T_tP$ phases.[2–6,15,16] The $\chi^{-1}(T)$ curves become progressively more bent towards the temperature axis with increasing t. At low substitution levels and above room temperature the $\chi^{-1}(T)$ curves are straight lines within the accuracy of the experimental technique. The composition at which the conversion from linear to bent

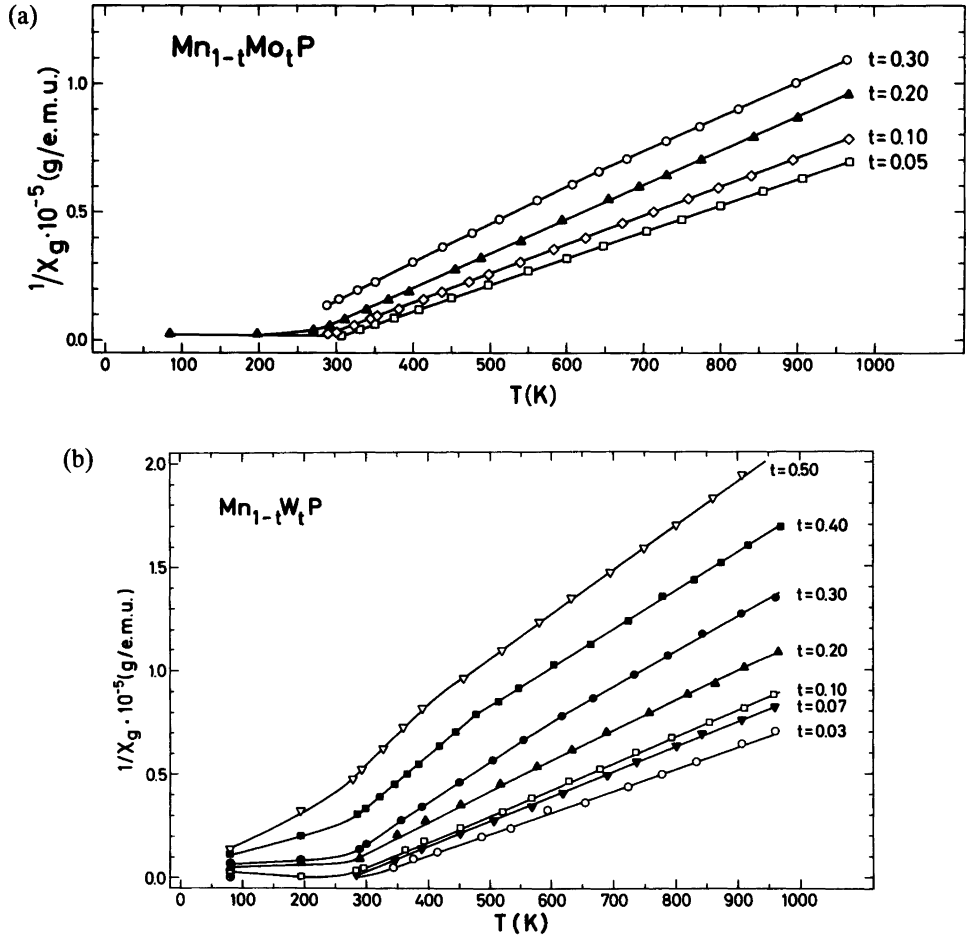

Fig. 3. Inverse magnetic susceptibility as function of temperature for (a) $Mn_{1-t}Mo_tP$ ($0.00 < t \leqq 0.30$) and (b) $Mn_{1-t}W_tP$ ($0.00 < t \leqq 0.50$).

Table 2. Weiss constant (θ), paramagnetic moment (μ_{eff}) and number of unpaired spins ($2S$) for $Mn_{1-t}Mo_tP$ ($0.00<t\leqq0.30$) and $Mn_{1-t}W_tP$ ($0.00<t\leqq0.50$).

T	t	θ (K)	μ_{eff} (μ_B per Mn,T)	$2S$ (per Mn,T)	Range (K)
Mo	0.05	280±10	2.61±0.05	1.79±0.04	310–1000
	0.10	270±10	2.52±0.05	1.72±0.04	290–1000
	0.20	250±10	2.38±0.05	1.58±0.04	290–1000
	0.30	200±10	2.27±0.10	1.48±0.08	275–650
		140±15	2.42±0.10	1.62±0.08	650–1000
W	0.03	285±10	2.64±0.05	1.82±0.04	320–1000
	0.05	280±10	2.59±0.05	1.77±0.04	300–1000
	0.07	270±10	2.52±0.05	1.72±0.04	290–1000
	0.10	260±10	2.50±0.05	1.70±0.04	290–1000
	0.20	235±10	2.37±0.10	1.57±0.08	290–650
		205±15	2.50±0.10	1.70±0.08	650–1000
	0.30	205±15	2.23±0.10	1.44±0.08	275–600
		150±15	2.42±0.10	1.62±0.08	600–1000
	0.40	160±20	2.15±0.15	1.37±0.12	275–450
		50±15	2.43±0.10	1.63±0.08	450–1000
	0.50	120±20	2.09±0.15	1.32±0.12	275–400
		20±15	2.38±0.10	1.58±0.08	400–1000

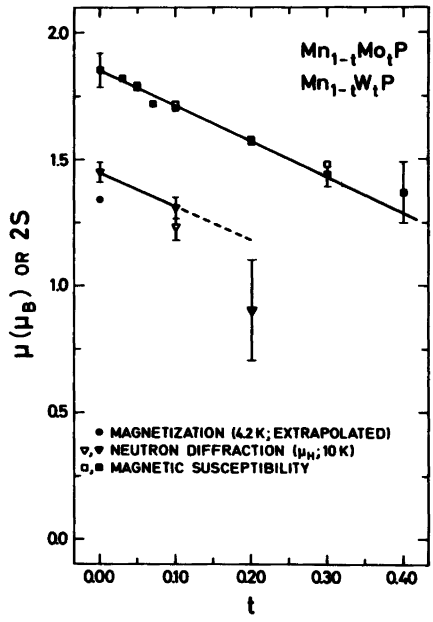

Fig. 4. Paramagnetic ("spin only") $2S$ and helimagnetic moment (μ_H) *versus* the compositional parameter t for $Mn_{1-t}Mo_tP$ (open symbols) and $Mn_{1-t}W_tP$. Legends to symbols are given on the illustration. Bars represent estimated or calculated errors.

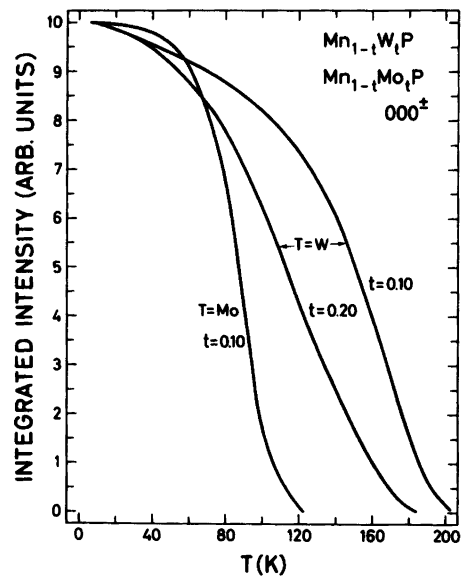

Fig. 5. Integrated intensity of $000^{\pm}$ *versus* temperature for $Mn_{0.90}Mo_{0.10}P$, $Mn_{0.90}W_{0.10}P$ and $Mn_{0.80}W_{0.20}P$. ($P\rightleftarrows H_c$ transitions in all cases.) Experimental points are omitted for clarity.

Table 3. Helimagnetic parameters for $Mn_{1-t}Mo_tP$ and $Mn_{1-t}W_tP$ at 10 K. (R_{spiral} ranging between 0.04 and 0.10; 6–12 magnetic satellite reflections.)

T	t	$\tau_c/2\pi c^*$	μ_H (μ_B)	$\phi_{1,2}$ (°)	T_N (K)
	0.00[a]	0.116±0.002	1.45±0.04	24±3	
Mo	0.10	0.117±0.004	1.23±0.06	30±3	105±10
W	0.10	0.168±0.003	1.32±0.04	35±5	195±10
	0.20	0.223±0.008	0.9 ±0.2	50±20	165±10

[a] T_C=292±4 K, μ_F=1.43(3)μ_B at 60 K, T_S=53±3 K.

characteristics is detectable differs somewhat with T [V ($0.15<t<0.20$),[3] Cr ($0.10<t<0.20$),[5,15] Fe ($0.28<t$),[4] Co ($0.30<t<0.40$)[14] and Ni ($0.10<t<0.20$)[6]], and $Mn_{1-t}Mo_tP$ ($0.20<t<0.30$) and $Mn_{1-t}W_tP$ ($0.10<t<0.20$) accordingly behave quite "normally" in this respect. The deviations from a single straight line for χ^{-1}(T) for higher substitution levels of Mo and W evidently was not observed by Guerin,[9] who reports linear χ^{-1}(T) characteristics up to t=0.95 for $Mn_{1-t}W_tP$. The small convex anomaly in the χ^{-1}(T) curves of $Mn_{1-t}Mo_tP$ near room temperature found by Guerin could not be substantiated in this study.

The χ^{-1}(T) curves in Fig. 3 are to a very good approximation described by one or two linear sections, *viz.* by one or two Curie-Weiss law relationships [$\chi^{-1}=C^{-1}(T-\theta)$]. Paramagnetic moment ($\mu_{eff}=\sqrt{8C_{mol}}$) and Weiss constant ($\theta$) as derived from the Curie-Weiss regions are listed in Table 2, together with the corresponding number of unparied spins ($2S$) according to the "spin only" approximation [$\mu_{eff}=g\sqrt{S(S+1)}$ with g=2]. The data derived from the "high temperature Curie-Weiss regions" are believed to have no simple physical interpretation and only those for the "low temperature regions" are considered below.

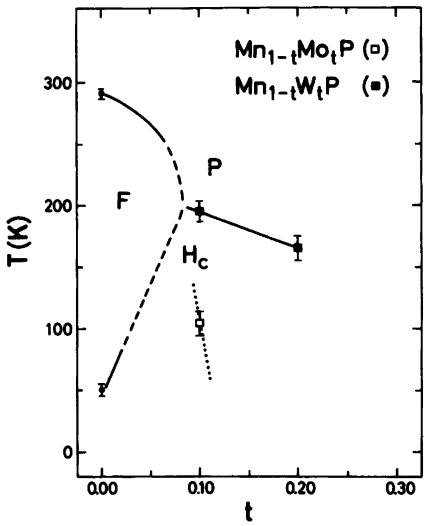

Fig. 6. Tentative sections of the magnetic phase diagrams for $Mn_{1-t}Mo_tP$ and $Mn_{1-t}W_tP$.

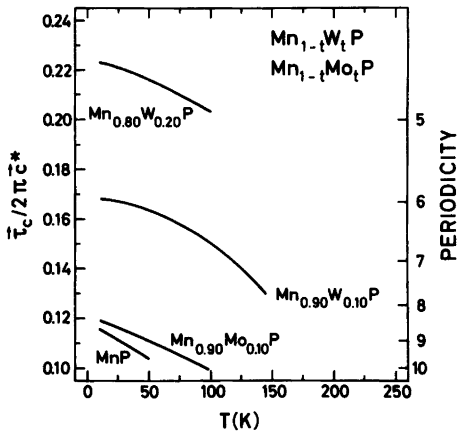

Fig. 7. Temperature dependences of the propagation vector (τ_c) for MnP, $Mn_{0.90}Mo_{0.10}P$, $Mn_{0.90}W_{0.10}P$ and $Mn_{0.80}W_{0.20}P$. Experimental points are omitted.

As for the other $Mn_{1-t}T_tP$ phases, θ, μ_{eff} and $2S$ (Table 2) decline with increasing t for $Mn_{1-t}Mo_tP$ and $Mn_{1-t}W_tP$. The corresponding parameter values for $Mn_{1-t}Mo_tP$ and $Mn_{1-t}W_tP$ agree within estimated error limits. The θ values listed in Table 2 are also in reasonable agreement with those derived from the $\chi^{-1}(T)$ curves of Guerin.[9] On the other hand, μ_{eff} of Guerin differ appreciably in value as well as in concentration dependence from the present findings. This discrepancy is intimately coupled to the distinction in the shape of the $\chi^{-1}(T)$ curves between Ref. 9 and Fig. 3 (*vide supra*).

The θ values for $Mn_{1-t}Mo_tP$ and $Mn_{1-t}W_tP$ with $0.00<t<\sim0.08$ are probably (*cf.* Refs. 2–6) some 10–30 K larger than the true Curie temperatures (T_C). The relation between $2S$ and the helimagnetic moment (μ_H) obtained by neutron diffraction [see (iii)] is shown in Fig. 4. As for the other $Mn_{1-t}T_tP$ phases,[2–6] the paramagnetic $2S$ values are considerably higher than the ordered moments. Also for $Mn_{1-t}Mo_tP$ and $Mn_{1-t}W_tP$ $2S$ and μ_H fall on approximately parallel lines which decline with increasing t. A more detailed discussion will be given in a forthcoming paper.

(iii) *Magnetic phase diagram and structures.* The present neutron diffraction results, which are limited to $Mn_{0.90}Mo_{0.10}P$, $Mn_{0.90}W_{0.10}P$ and $Mn_{0.80}W_{0.20}P$, did not show any sign of the F phase characteristic of MnP itself. These samples convert directly to the H_c state and the $P \rightleftarrows H_c$ phase transition is almost certainly of second (or higher) order. No indication of hysteresis is, *e.g.*, observed in the temperature variation of the integrated intensity of the $000^{\pm}$ satellites for the samples (Fig. 5). In line with the findings[2–6] for the $Mn_{1-t}T_tP$; $T=3d$ metal phases, the temperature characteristics in Fig. 5 are rather broad. The scarce reliable data for the magnetic transformation temperatures are rationalized into the tentative magnetic phase diagrams for $Mn_{1-t}Mo_tP$ and $Mn_{1-t}W_tP$ in Fig. 6. The prominent feature of Fig. 6 is that the P,F and H_c phases evidently meet in triple points, and $Mn_{1-t}Mo_tP$ and $Mn_{1-t}W_tP$ accordingly resemble $Mn_{1-t}Fe_tP$[4] in this respect. We suggest that the triple point is located at $t\approx0.08$ and $T\approx200$ K for $Mn_{1-t}W_tP$ whereas we hesitate to give values for $Mn_{1-t}Mo_tP$. A more detailed exploration of these magnetic phase diagrams by other suitable methods is in progress.

The original model[17,18] for the magnetic structure of the H_c phase of MnP is used because this has proved to provide a reasonable approximation to the $Mn_{1-t}T_tP$; $T=3d$ metal phases.[1–6] Numerical values for the variable parameters of the model (*viz.* the propagation vector τ_c of the spirals, the helimagnetic moment μ_H and the phase angle $\phi_{1,2}$ between the spirals through atoms 1 and 2, *cf.* Ref. 11) are given in Table 3 together with the corresponding results for MnP (powder data, *cf.* the discussion in Ref. 2).

The compositional variations of τ_c, μ_H and $\phi_{1,2}$ at 10 K (Table 3) appear to bring out a distinction between $Mn_{1-t}Mo_tP$ and $Mn_{1-t}W_tP$ in that the former shows less compositional variations in τ_c and $\phi_{1,2}$ than the latter. However, additional data for both phases are needed in order to confirm this, but independent of the outcome $Mn_{1-t}Mo_tP$ and $Mn_{1-t}W_tP$ will fit into the general picture of the $Mn_{1-t}T_tP$ phases.[1–6]

The temperature dependences of τ_c for MnP, $Mn_{0.90}Mo_{0.10}P$, $Mn_{0.90}W_{0.10}P$ and $Mn_{0.80}W_{0.20}P$ are shown in Fig. 7. μ_H decreases with increasing T and becomes zero at T_N. Due to the close coupling between μ_H and $\phi_{1,2}$ the situation for $\phi_{1,2}$ is less clear, but the present data suggest that $\phi_{1,2}$ is an essentially temperature independent parameter for $Mn_{1-t}Mo_tP$ and $Mn_{1-t}W_tP$. Also in these respects $Mn_{1-t}Mo_tP$ and $Mn_{1-t}W_tP$ fit into the pattern of the $Mn_{1-t}T_tP$ phases which we have studied.

REFERENCES

1. Fjellvåg, H., Kjekshus, A., Zięba, A. and Foner, S. *J. Phys. Chem. Solids 45* (1984) 709.
2. Fjellvåg, H. and Kjekshus, A. *Acta Chem. Scand. A 38* (1984) 563.
3. Fjellvåg, H. and Kjekshus, A. *Acta Chem. Scand. A 38* (1984) 703.
4. Fjellvåg, H., Kjekshus, A. and Andresen, A.F. *Acta Chem. Scand. A 38* (1984) 711.
5. Fjellvåg, H., Kjekshus, A. and Andresen, A.F. *Acta Chem. Scand. A 39* (1985) 143.
6. Fjellvåg, H. and Kjekshus, A. *Acta Chem. Scand. A 38* (1984) 719.
7. Rundqvist, S. and Lundström, T. *Acta Chem. Scand. 17* (1963) 37.
8. Rundqvist, S. *Acta Chem. Scand. 16* (1962) 287.
9. Guerin, R. *Thesis,* University of Rennes, Rennes 1976.
10. Guerin, R. and Sergent, M. *C. R. Acad. Sci. Ser. C 281* (1975) 777.
11. Fjellvåg, H. and Kjekshus, A. *Acta Chem. Scand. A 38* (1984) 1.
12. Bacon, G.E. In Yelon, W.B., Ed., *Neutron Diffraction Newsletter,* Columbia 1977.
13. Watson, R.E. and Freeman, A.J. *Acta Crystallogr. 14* (1961) 27.
14. Bonnerot, J., Fruchart, R. and Roger, A. *Phys. Lett. A 26* (1968) 536.
15. Selte, K., Birkeland, L. and Kjekshus, A. *Acta Chem. Scand. A 32* (1978) 731.
16. Selte, K., Fjellvåg, H. and Kjekshus, A. *Acta Chem. Scand. A 33* (1979) 391.
17. Felcher, P.G. *J. Appl. Phys. 37* (1966) 1056.
18. Forsyth, J.B., Pickart, S.J. and Brown, P.G. *Proc. Phys. Soc. 88* (1966) 333.

Received August 4, 1984.